Table III. X-ray Crystallographic Data for $Ln_{1/3}UO_2PO_4 \cdot nH_2O$ (Cu $K\alpha_1$, $K\alpha_2$; λ = 1.5418 Å; 20 °C; Z = 4)

compd[a]	color	fw	a, Å	c, Å
$La_{1/3}UO_2PO_4 \cdot 4.7H_2O$	yellow	495.90	6.966 (5)	22.36 (8)
$Pr_{1/3}UO_2PO_4 \cdot 4.7H_2O$	pale yellow-green	496.57	6.970 (7)	22.23 (8)
$Nd_{1/3}UO_2PO_4 \cdot 4.3H_2O$	pale yellow-orange	490.48	6.986 (6)	22.08 (9)

[a] All compounds belong to the tetragonal system.

rotational oscillations remain, restricted by strong interactions with the neighboring atoms.[16]

The X-ray diffraction of the lanthanide uranyl phosphates can be indexed in the tetragonal system. Table III contains the crystallographic data of these solids.

The diffuse-reflectance spectra reveal that the absorption maxima of the LnUP hydrates are similar to the absorption spectra of the hydrated salts of the lanthanides and of the ions present in the aqueous solutions.[17] Figure 4 shows the LaUP, PrUP, and NdUP spectra. The lanthanum derivative does not show absorption maxima in the visible region, as is appropriate for a metallic ion with a complete electron shell; the uranyl group vibration bands, however, appear to be attenuated, probably because of the interaction between the uranyl group and $La(OH_2)_n^{3+}$. Olken et al.[1] also report alterations in the emission characteristics of the uranyl phosphates when they contain several intercalated ions, but the behavior observed in the present work could correspond to any correlation and further investigation is required to classify the system.

(15) Baran, E. J.; Botto, I. L. *Monatsh. Chem.* **1977**, *108*,, 781.
(16) Van der Elsken, J.; Robinson, D. W. *Spectrochim. Acta* **1961**, *17*, 1249.
(17) Moeller, T. In *Comprehensive Inorganic Chemistry*; Bailar, J. C., Jr., Ed.; Pergamon: Oxford, U.K., 1973; Vol. 4.

Conclusion

HUP and BAUP are formed by $(UO_2PO_4)_n^{n-}$ layers, which can be easily separated to permit the intercalation of ions by the respective exchange of H_3O^+ and $C_4H_9NH_3^+$ cations. The pH of the exchange media must be carefully controlled to avoid the hydrolysis of the host compound to that precipitation of insoluble and highly stable lanthanide orthophosphate does not occur. The lanthanide acetate solutions provide a buffer media appropriate to prevent host dissolution. The ionic interdiffuison mechanism proposed by Howe[9] is in agreement with the evolution of the X-ray diffractograms and IR spectra of the exchange process. The retention of Ln_{aq}^{3+} ions is caused by a topotactic process because the *ab* plane is preserved during intercalation.

Acknowledgment. We thank the CAICYT (Ministry of Education and Science, Spain) for financial support. We are also grateful to David W. Schofield for reviewing the English version.

Registry No. $La(UO_2PO_4)_3 \cdot 14H_2O$, 107453-28-1; $Pr(UO_2PO_4)_3 \cdot 14H_2O$, 107453-29-2; $Nd(UO_2PO_4)_3 \cdot 13H_2O$, 107453-30-5; $H_3O(UO_2PO_4) \cdot 3H_2O$, 107453-31-6; $C_4H_9NH_3(UO_2PO_4) \cdot 3H_2O$, 102566-09-6; La, 7439-91-0; Pr, 7440-10-0; Nd, 7440-00-8; $(H_3O)_3Nd(UO_2PO_4)_6 \cdot xH_2O$, 107453-32-7.

Supplementary Material Available: Listings of observed and calculated *d* spacings, relative intensities, and Miller indices from the X-ray powder diffraction diagram (6 pages). Ordering information is given on any current masthead page.

Contribution from the ISSECC, CNR, Firenze, Italy, and Departments of Chemistry, University of Modena, Modena, Italy, and University of Firenze, Firenze, Italy

Anisotropic Exchange in Dinuclear Complexes with Polyatomic Bridges. Crystal and Molecular Structure and EPR Spectra of (μ-Oxalato)bis(1,10-phenanthroline)dicopper(II) Dinitrate

Alessandro Bencini,*[1a] Antonio C. Fabretti,[1b] Claudia Zanchini,[1c] and Paolo Zannini[1b]

Received July 31, 1986

The X-ray crystal structure of (μ-oxalato)bis(1,10-phenanthroline)dicopper(II) dinitrate was determined at room temperature. The crystals are triclinic, space group $P\bar{1}$, with a = 9.977 (6) Å, b = 9.658 (6) Å, c = 7.036 (3) Å, α = 108.03 (4)°, β = 95.40 (4)°, γ = 90.22 (4)°, and Z = 2. The least-squares refinement of the structure led to a conventional R factor of 0.036. Single-crystal EPR spectra were recorded at X-band (9-GHz) frequency at 77 K. The measured zero-field splitting tensor was found to be largely misaligned from the **g** tensor, showing that exchange contributions to the anisotropic spin–spin interaction are operative. The relative influences of the dipolar magnetic and the anisotropic exchange interactions in determining the zero-field splitting in oxalato-bridged copper(II) dimers are discussed.

Introduction

Anisotropic exchange interactions between couples of transition-metal ions have been extensively studied in the last few years since they allow one to estimate exchange interactions between ground and excited states of the dinuclear unit.[2] The mechanisms that determine the anisotropic exchange interactions[3] are not related to those responsible for the isotropic exchange interaction, which often control the magnetic properties of dinuclear species, and involve exchange interactions between the ground states of the magnetic ions.[4,5] As a matter of fact, in a series of μ-hydroxo-bridged copper(II) complexes the isotropic exchange coupling between the unpaired electrons can be ferro- or antiferromagnetic according to the value of the Cu–O–Cu bridging angle[4] while the anisotropic magnetic interaction remains always ferromagnetic.[6]

Dinuclear copper(II) complexes are still the simplest systems to investigate, and since they can be found in a number of different geometries, they are ideal candidates for systematic investigations on correlations between structural and magnetic parameters. The anisotropic exchange interactions in copper(II) couples determine, together with direct magnetic interactions,[3] the zero-field splitting of the triplet state arising from the isotropic exchange interactions

(1) (a) ISSECC, CNR. (b) University of Modena. (c) University of Firenze.
(2) Gatteschi, D.; Bencini, A. In *Magneto-Structural Correlations in Exchange-Coupled Systems*; Willet, R. D., Gatteschi, D., Kahn, O., Eds.; D. Reidel: Dordrecht, Holland, 1984; p 241.
(3) Owen, J.; Harris, E. A. In *Electron Paramagnetic Resonance*; Geschwind, S., Ed.; Plenum: New York, 1972; p 427.
(4) Hay, P. J.; Thibeault, J. C.; Hoffmann, R. *J. Am. Chem. Soc.* **1975**, *97*, 4884.
(5) Kahn, O.; Briat, B. *J. Chem. Soc., Faraday Trans. 2* **1976**, *72*, 268, 1441.
(6) Banci, L.; Bencini, A.; Gatteschi, D. *J. Am. Chem. Soc.* **1983**, *105*, 761.

0020-1669/87/1326-1445$01.50/0

and can in principle give measurable effects on the EPR spectra.

The zero-field splittings measured in a series of dinuclear μ-oxo- and μ-chloro-bridged copper(II) complexes[2,6-11] were found to be determined by magnetic dipolar interactions and ferromagnetic exchange interactions between the ground $|xy\rangle$ and the excited $|x^2-y^2\rangle$ type molecular orbitals. With the notation $|i\rangle$ we indicate a LCAO molecular orbital whose largest contribution is given by the $|i\rangle$ atomic orbital. It must be anticipated that orbital mixing caused by the low symmetry of the complexes has important effects on the zero-field splitting. The magnitude of the exchange interaction varies from 200–300 to 10–30 cm^{-1} along the series and decreases when the internuclear copper(II)–copper(II) distance is increased. This behavior was rationalized by using a semiempirical approach,[12] and quantitative estimates of anisotropic exchange interactions still constitute challenges to theoretical chemists.

As the size of the groups bridging the two copper atoms was increased, it was found that the exchange contributions to the zero-field splitting decrease. In bis(μ-1,3-azido)bis(1,1,4,7,7-pentamethyldiethylenetriamine)dicopper(II) bis(tetraphenylborate) a singlet–triplet splitting of 13 cm^{-1} was observed and an anisotropic exchange contribution around 50 cm^{-1} was estimated.[9] Measurable anisotropic exchange of the order of a few reciprocal centimeters was observed in the (μ-benzotriazolato-N^1,N^2)bis[[tris((N^1-methylbenzimidazol-2-yl)methyl)amine-$N,N^3,N^{3'},N^{3''}$]copper(II)] trinitrate complex, where the copper(II) atoms are 5.536 Å apart and a singlet–triplet splitting of 24 cm^{-1} was observed.[10]

Oxalato, oxamidato, and oxamato molecules have been found to be very effective in transmitting exchange interactions, and singlet–triplet separations ranging from 300 to 500 cm^{-1} have been observed in dinuclear copper(II) species.[14-20] The EPR spectra of some copper(II) complexes with oxalato, oxamidato, and oxamato bridges have been recently reported.[13] All the spectra showed zero-field splitting effects, but intermolecular exchange interactions made any accurate analysis impossible. However, the measured zero-field splittings were nicely reproduced by taking into account only magnetic dipolar interactions, and it was concluded that anisotropic exchange effects in these complexes are negligible.

We have recently been able to crystallize the complex (μ-oxalato)bis(1,10-phenanthroline)dicopper(II) dinitrate, $[Cu_2(phen)_2(C_2O_4)(NO_3)_2]$, previously studied as a polycrystalline powder,[13] and we have measured nicely resolved EPR spectra at 77 K. Since these spectra showed effects that could be due to sizable anisotropic exchange effects, we decided to fully investigate the structure and magnetic properties of this complex.

We wish to report here the crystal and molecular structure and the single-crystal EPR spectra of $[Cu_2(phen)_2(C_2O_4)(NO_3)_2]$ with the aim of obtaining a fuller insight into the nature of the exchange interactions involving ground and excited orbitals.

Table I. Summary of Crystal Data, Intensity Collection, and Structure Refinement

formula	$C_{13}H_8N_3O_5Cu$
fw	349.77
space group	$P\bar{1}$
a, Å	9.977 (6)
b, Å	9.658 (6)
c, Å	7.036 (3)
α, deg	108.03 (4)
β, deg	95.40 (4)
γ, deg	90.22 (4)
V, Å^3	641.5
Z	2
cryst size, mm	0.18 × 0.20 × 0.24
μ(Mo Kα), cm^{-1}	17.32
scan type	ω–2θ
scan width, deg	1.5
scan speed, deg min^{-1}	4.5
2θ limits, deg	5–50
data collection range	$\pm h,\pm k,+l$
no. of data	2267
no. of data $F_o^2 > 3.5\sigma(F_o^2)$	2216
R	0.036
R_w	0.040

Table II. Positional Parameters for the Non-Hydrogen Atoms (Esd's in Parentheses)[a]

atom	x	y	z
Cu	1765 (2)	2009 (2)	1984 (1)
O(1)	1687 (2)	9857 (2)	764 (3)
O(2)	9809 (2)	1857 (2)	1122 (3)
O(3)	1421 (2)	2316 (3)	5153 (3)
O(4)	2819 (3)	637 (3)	5270 (4)
O(5)	1873 (4)	1787 (4)	7877 (4)
N(1)	3767 (2)	2206 (2)	2219 (3)
N(2)	1901 (2)	4146 (3)	2315 (4)
N(3)	1996 (3)	1537 (3)	6086 (4)
C(1)	4682 (3)	1205 (3)	2229 (4)
C(2)	6061 (3)	1494 (3)	2277 (5)
C(3)	6510 (3)	2849 (4)	2350 (5)
C(4)	5566 (3)	3947 (3)	2391 (4)
C(5)	5913 (3)	5420 (3)	2516 (4)
C(6)	4954 (3)	6419 (3)	2554 (4)
C(7)	3557 (3)	6035 (3)	2477 (4)
C(8)	3193 (3)	4612 (3)	2370 (4)
C(9)	4203 (3)	3557 (3)	2315 (4)
C(10)	2501 (3)	7012 (3)	2527 (5)
C(11)	1210 (3)	6539 (4)	2486 (5)
C(12)	938 (3)	5102 (3)	2391 (5)
C(13)	9461 (3)	575 (3)	104 (4)

[a] Coordinates multiplied by 10^4.

Experimental Section

Synthesis of the Complex. $[Cu_2(phen)_2(C_2O_4)(NO_3)_2]$ was prepared by adding to 15 mL of a water solution of 2 mmol of $Cu(NO_3)_2{\cdot}3H_2O$ and 2 mmol of 1,10-phenanthroline 4 mL of a water solution of 1 mmol of $Na_2C_2O_4$. Single crystals were grown by slow evaporation of water solutions at 25 °C. Blue single crystals of the title compound were collected after 2 months. If the recrystallization is carried out in an acetonitrile/methanol/water (1:4:3) mixture, the monomeric $[Cu(phen)C_2O_4{\cdot}H_2O]H_2O$[21] complex is obtained.

X-ray Structural Determination. Single-crystal diffraction data for $[Cu_2(phen)_2(C_2O_4)(NO_3)_2]$ were collected at room temperature on a Philips PW 1100 automated diffractometer using graphite-monochromated Mo Kα radiation (λ = 0.7107 Å). Details on crystal data, intensity collection, and refinement are reported in Table I.

The positions of all non-hydrogen atoms were obtained by the usual Patterson and Fourier methods. Scattering factors and anomalous dispersion corrections for neutral atoms were employed;[22] all the calculations were performed on a Gould CSD MPX-32 computer using the SHELX-76 program system[23] and the ORTEP plotting program[24] for drawings. The

(7) Bencini, A.; Gatteschi, D.; Zanchini, C. *Inorg. Chem.* **1985**, *24*, 700, 704.
(8) Banci, L.; Bencini, A.; Gatteschi, D.; Zanchini, C. *J. Magn. Reson.* **1982**, *48*, 9.
(9) Banci, L.; Bencini, A.; Gatteschi, D. *Inorg. Chem.* **1984**, *23*, 2138.
(10) Bencini, A.; Gatteschi, D.; Reedijk, J.; Zanchini, C. *Inorg. Chem.* **1985**, *24*, 207.
(11) Boillot, M. L.; Journaux, Y.; Bencini, A.; Gatteschi, D.; Kahn, O. *Inorg. Chem.* **1985**, *24*, 263.
(12) Charlot, M. F.; Journaux, Y.; Kahn, O.; Bencini, A.; Gatteschi, D.; Zanchini, C. *Inorg. Chem.* **1986**, *25*, 1060.
(13) Bencini, A.; Benelli, C.; Gatteschi, D.; Zanchini, C.; Fabretti, A. C.; Franchini, G. C. *Inorg. Chim. Acta* **1984**, *86*, 169.
(14) Julve, M.; Verdaguer, M.; Kahn, O.; Gleizes, A. *Inorg. Chem.* **1983**, *22*, 368.
(15) Michalowicz, A.; Girerd, J. J.; Goulon, J. *Inorg. Chem.* **1979**, *18*, 3004.
(16) Girerd, J. J.; Kahn, O.; Verdaguer, M. *Inorg. Chem.* **1980**, *19*, 274.
(17) Felthouse, T. R.; Laskowski, E. J.; Hendrickson, D. N. *Inorg. Chem.* **1977**, *16*, 1077.
(18) Girerd, J. J.; Jeannin, S.; Jeannin, Y.; Kahn, O. *Inorg. Chem.* **1978**, *17*, 3034.
(19) Chauvel, C.; Girerd, J. J.; Jeannin, Y.; Kahn, O.; Lavigne, J. *Inorg. Chem.* **1979**, *18*, 3015.
(20) Bencini, A.; DiVaira, M.; Fabretti, A. C.; Gatteschi, D.; Zanchini, C. *Inorg. Chem.* **1984**, *23*, 1620.
(21) Fabretti, A. C.; Franchini, G. C.; Zannini, P.; DiVaira, M. *Inorg. Chim. Acta* **1985**, *105*, 187.
(22) *International Tables for X-ray Crystallography*; Kynoch: Birmingham, England, 1974; Vol. IV.

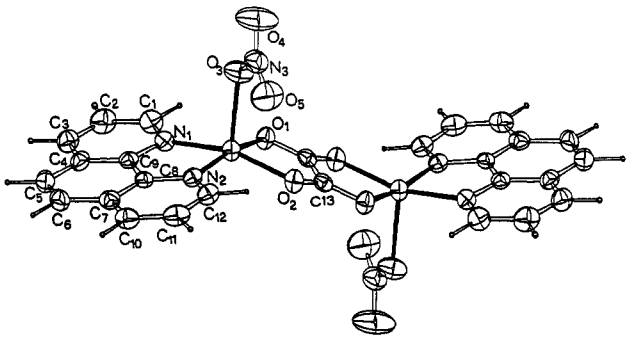

Figure 1. ORTEP view of the molecule $[Cu_2(phen)_2(C_2O_4)(NO_3)_2]$.

Table III. Most Significative Bond Distances (Å) and Bond Angles (deg) (Esd's in Parentheses)

Cu–N(1)	1.991 (2)	N(3)–O(3)	1.251 (4)
Cu–N(2)	2.006 (2)	N(3)–O(4)	1.243 (4)
Cu–O(1)	1.987 (2)	N(3)–O(5)	1.226 (4)
Cu–O(2)	1.980 (2)	Cu–Cu′	5.158 (3)
Cu–O(3)	2.216 (2)		
N(1)–Cu–N(2)	82.5 (1)	O(3)–Cu–N(1)	100.7 (1)
N(1)–Cu–O(1)	95.2 (1)	O(3)–Cu–N(2)	94.9 (1)
N(1)–Cu–O(2)	166.6 (1)	O(3)–Cu–O(1)	103.2 (1)
N(2)–Cu–O(2)	93.5 (1)	O(3)–Cu–O(2)	92.3 (1)
N(2)–Cu–O(1)	161.9 (1)	O(3)–N(3)–O(4)	119.9 (3)
O(1)–Cu–O(2)	84.6 (1)	O(3)–N(3)–O(5)	119.7 (3)
		O(4)–N(3)–O(5)	119.8 (3)

structure was refined with use of a full-matrix least-squares method based on minimization of the function $\sum w(|F_o| - |F_c|)^2$ with weights $w = 1/\sigma^2(F_o)$. Anisotropic thermal parameters were used for all the non-hydrogen atoms. Hydrogen atoms were introduced in calculated positions (C–H = 1.08 Å) as fixed contributions to F_c, each with a temperature factor ca. 20% larger than the isotropic equivalent of the respective carbon atom. The final values of the discrepancy indices, defined by $R = \sum[|F_o| - |F_c|]/\sum|F_o|$ and $R_w = [\sum w(|F_o| - |F_c|)^2/\sum w(F_o)^2]^{1/2}$, were $R = 0.036$ and $R_w = 0.040$. The highest peaks in the last difference Fourier map calculated at the end of the refinement were less than 0.4 e Å^{-3}. Final atomic positional parameters for the nonhydrogen atoms are listed in Table II. Thermal parameters and positional parameters for the hydrogen atoms are listed in Tables SI and SII, respectively. A listing of the observed and calculated structure amplitudes is available as supplementary material.

EPR Spectra. Single crystals suitable for EPR spectroscopy were oriented with a Philips PW 1100 automatic diffractometer. The crystals used in the experiment showed well-developed (001) and (0,0,−1) faces. Polycrystalline powder and single-crystal X-band (9.1-GHz) spectra and polycrystalline Q-band (35-GHz) powder spectra were recorded on a Varian E-9 spectrometer at 133 K using the apparatus previously described.

Results and Discussion

Description of the Structure. A drawing of the dimer structure, showing the labeling scheme of the asymmetric unit, is given in Figure 1; selected bond distances and angles are reported in Table III.

The structure consists of centrosymmetric $[Cu_2(phen)_2(C_2O_4)(NO_3)_2]$ molecules. Each copper atom is in a square-pyramidal coordination with N(1), N(2), O(1), and O(2) in the basal plane and O(3) from a nitrato group coordinated in the axial position at 2.216 (2) Å. The bidentate phenanthroline molecule is planar (root mean square deviation of atoms 0.013 Å), and the plane of the phenanthroline makes a 15.2° angle with the basal N(1)N(2)O(1)O(2) coordination plane. The planar oxalato group bridges the two copper atoms in the usual way, each copper atom being bound to two oxygens from the two different carboxylic groups. The copper–copper distance is 5.158 (1) Å, one of the shortest distances ever found for this class of compounds. The copper atoms are significantly displaced from basal planes (0.271 (2) Å) toward the nitro oxygen atom O(3). All relevant parameters of 1,10-phenanthroline and oxalato molecules are in good accord with previously obtained data for the monomeric molecule[21] and literature reports.[14,17,25-30]

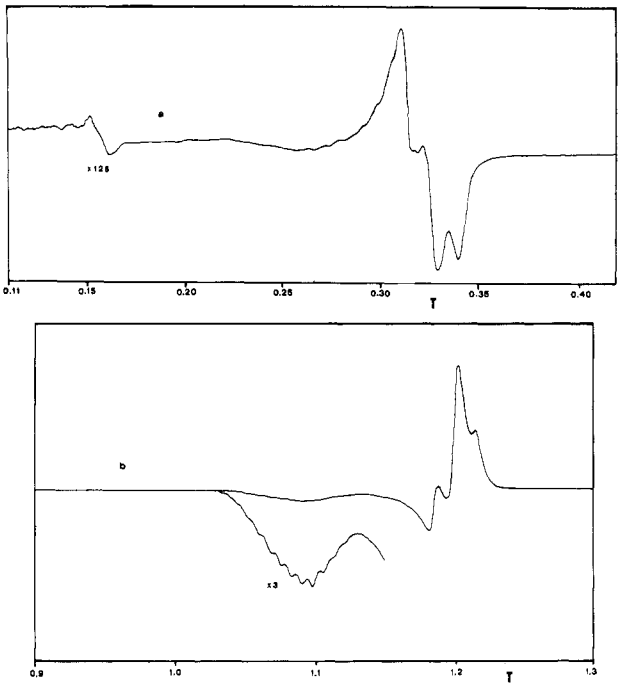

Figure 2. Polycrystalline powder EPR spectra of $[Cu_2(phen)_2(C_2O_4)(NO_3)_2]$ recorded at 133 K: (a) X-band; (b) Q-band.

Particularly, "bite" angles of 1,10-phenanthroline and oxalate are 82.5 (1) and 84.6 (1)°, respectively, in good accord with the expected ones.

The tetragonality parameter[31,32] for the copper coordination sphere is $T = 0.897$, identifying a tendency to square-planar arrangement, typical of the weak interaction with NO_3^-. There is no evidence of elongation in the N–O bond, due to copper interaction, and the apical position is quite regular, bearing only a slight distortion toward the N(1)–O(1) side: N(1)–Cu–O(3) = 100.7°, O(1)–Cu–O(3) = 103.2°.

EPR Spectra. Polycrystalline powder EPR spectra of $[Cu_2(phen)_2(C_2O_4)(NO_3)_2]$ were recorded at X- and Q-band at room temperature and at 133 K. The spectra recorded at 133 K are shown in Figure 2. These spectra are better resolved than the room-temperature ones and show resolved hyperfine splitting due to the coupling of the unpaired electrons with two equivalent copper nuclei. The spectra are characteristic of a triplet spin state with an anisotropic zero-field splitting tensor, and we tried to fit them using the reported formulas for the transition fields along the principal axes.[33] No reasonable fitting was obtained, suggesting the existence of noncollinear **g** and **D** tensors. This hypothesis was confirmed by the single-crystal analysis.

Single-crystal spectra have been recorded at X-band at 133 K by rotating the crystal with respect to the magnetic field along

(23) Sheldrick, G. M. *SHELX 76 System of Computing Programs*; University of Cambridge: Cambridge, England, 1976.
(24) Johnson, C. K. *Oak Ridge Natl. Lab., [Rep.] ORNL (U.S.)* **1965**, *ORNL-3794*.
(25) Nishigaki, S.; Yoshioka, H.; Nakatsu, K. *Acta Crystallogr., Sect. B: Struct. Crystallogr. Cryst. Chem.* **1978**, *B34*, 875.
(26) Lim, M. C.; Sinn, E.; Martin, R. B. *Inorg. Chem.* **1976**, *15*, 807.
(27) Stephen, F. S. *J. Chem. Soc. A* **1969**, 2493.
(28) Escobar, C.; Wittke, O. *Acta Crystallogr., Sect. C: Cryst. Struct. Commun.* **1983**, *C39*, 1643.
(29) Simmons, C. J.; Seff, K.; Cufford, F.; Hathaway, B. J. *Acta Crystallogr., Sect. C: Cryst. Struct. Commun.* **1983**, *C39*, 1360.
(30) Julve, M.; Faus, J.; Verdaguer, M.; Gleizes, A. *J. Am. Chem. Soc.* **1984**, *106*, 8306.
(31) Roos, B. *Acta Chem. Scand.* **1966**, *20*, 1673.
(32) Fitzgerald, W.; Foley, J.; McSweeney, D.; Ray, N.; Sheahan, D.; Tyagi, S.; Hathaway, B.; O'Brien, P. *J. Chem. Soc., Dalton Trans.* **1982**, 1117.
(33) Wasserman, E.; Snyder, L. C.; Yager, W. A. *J. Chem. Phys.* **1964**, *41*, 1763.

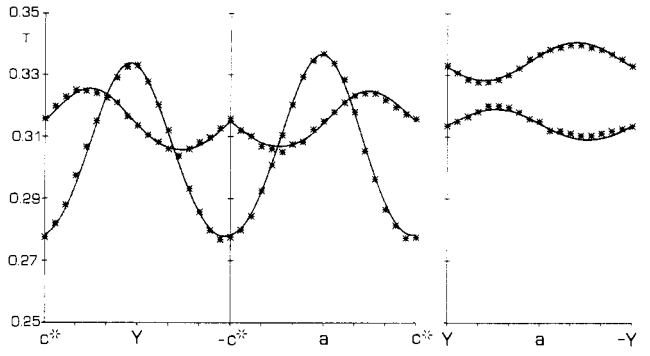

Figure 3. Angular dependence of the transition fields for $[Cu_2(phen)_2(C_2O_4)(NO_3)_2]$ recorded at X-band at 133 K.

the orthogonal $x = a$, y and $z = c^*$ axes. Since $\gamma = 90.2°$, y is actually making a 0.2° angle with b. This value is well below the experimental error, and y can be assumed to be parallel to b. Since only one molecule is present in the unit cell, two signals at most were observed at each crystal setting, which correspond to the $\Delta M_S = \pm 1$ transitions. In some positions the forbidden $\Delta M_S = \pm 2$ transition was observed at half field split into seven lines separated by ~8 mT.

The angular dependence of the $\Delta M_S = \pm 1$ transition fields in the ay, yc^*, and c^*a planes is shown in Figure 3. The best-fit curves, calculated through the nonlinear least-squares procedure previously described,[8] are also shown in Figure 3. The data have been fitted to the spin Hamiltonian $\mathcal{H} = \mu_B \mathbf{B}\cdot\mathbf{g}\cdot\mathbf{S} + \mathbf{S}\cdot\mathbf{D}\cdot\mathbf{S}$.

In crystal orientations near the c^* crystal axis, a seven-line hyperfine structure was observed in the $\Delta M_S = \pm 1$ transitions with the maximum splitting of 8.2 mT. As one goes away from c^*, the line separation decreases until the seven lines merged under the line width. Since we could observe the hyperfine splitting only in a limited angular range, we did not measure the **A** tensor. The direction of maximum splitting is, however, parallel to g_z, within experimental error, and we can say that **A** and **g** are parallel with $A_{\parallel} = 87 \times 10^{-4}$ cm^{-1}.

The best-fit spin Hamiltonian parameters and the computed standard deviations are reported in Table IV. The **g** directions in the xy plane are affected by a large experimental error since, the **g** tensor being quasi-axial ($g_{xx} = 2.060$ (2), $g_{yy} = 2.068$ (2)), the angular dependence of the transition fields in this plane is almost totally due to the zero-field splitting. The computed y direction makes an angle of 3° with the C(13)–C(13)′ bond direction, which should be one principal axis in the idealized C_{2h} symmetry of the molecule (point symmetry on each copper center σ_h). In the fitting procedure ambiguity exists in the sign of the principal values of the **D** tensor, which depends on the assignment of the $|1\rangle$ and $|-1\rangle$ levels (strong-field labeling). This ambiguity cannot be resolved by EPR spectra. In Table IV the two possible choices of sign are explicitly shown.

The **g** and **D** tensors are not collinear. The angle between g_{zz} and $D_{z'z'}$ is 27 (1)°, the angle between g_{xx} and $D_{x'x'}$ is 28 (5)°, and $D_{y'y'}$ makes an angle of 5° with C(13)–C(14) and 7 (5)° with g_{yy}. The relative orientation of **g** and **D** with respect to the molecule is shown in Figure 4. g_{zz} makes an angle of 10° with the axial Cu–O(3) bond direction.

The zero-field splitting **D** for a copper(II)–copper(II) couple is determined by two main contributions:[6] a direct magnetic interaction between the unpaired spins (often taken as magnetic dipolar interaction) and a superexchange interaction. The magnetic dipolar interaction is represented in a spin Hamiltonian formalism by the symmetric tensor $\mathbf{D}^d$, which can be easily computed in the **g** principal axis system. Upon diagonalization we obtain the principal values and directions. $D^d_{xx} = -0.0140$ cm^{-1}, $D^d_{yy} = 0.0063$ cm^{-1}, and $D^d_{zz} = 0.0077$ cm^{-1}; x is parallel to the Cu–Cu direction and z makes an angle of 16° with g_z. $\mathbf{D}^d$ compares well with the dipolar tensor computed[20] for $Cu_2L(BPh_4)_2\cdot 2CH_3CO$ (L = μ-*N*,*N*′-bis(6-ethyl-3,6-diazaoctyl)oxamidato(2−)-N^1,N^3,N^6,O:$N^{1\prime}$,$N^{3\prime}$,$N^{6\prime}$,$O^{\prime}$), which was used to interpret the EPR spectra, and it must also be noted that D^d_{xx} is equal to the largest value of the observed zero field splitting $D_{z'z'}$. It is apparent, however, that $\mathbf{D}^d$ cannot account for **D** since $D_{z'z'}$ has been found 47° away from the Cu–Cu direction and $D_{y'y'}$ is comparable in magnitude with $D_{z'z'}$, the largest principal value.

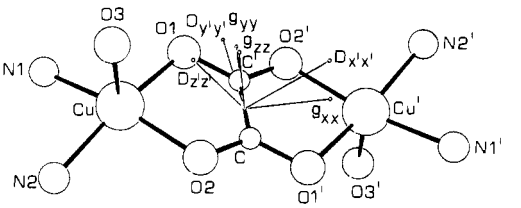

Figure 4. Orientation of the **g** and **D** tensors with regard to the dinuclear unit.

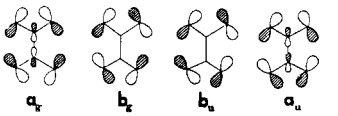

Figure 5. Schematic representation of the HOMO's of the oxalato molecule labeled according to the C_{2h} irreducible representations.

Table IV. Best-Fit Spin Hamiltonian Parameters for $[Cu_2(phen)_2(C_2O_4)(NO_3)_2]$[a]

$g_{xx} = 2.060$ (2)	$g_{yy} = 2.068$ (2)	$g_{zz} = 2.285$ (2)
0.7 (1)	0.6 (1)	0.104 (8)
0.6 (1)	−0.7 (1)	0.264 (8)
0.26 (2)	−0.12 (4)	−0.959 (2)
$D_{x'x'} = \pm 0.0036$ (2)	$D_{y'y'} = \pm 0.0104$ (2)	$D_{z'z'} = \mp 0.0140$ (1)
0.60 (1)	−0.77 (1)	−0.193 (1)
0.77 (1)	0.63 (1)	−0.093 (1)
−0.19 (1)	0.09 (1)	−0.977 (2)

[a] Estimated standard deviations on the last significant digits are given in parentheses. The x, y, z and x', y', z' axes are defined in the text.

Under the assumption that $\mathbf{D} = \mathbf{D}^d + \mathbf{D}^{ex}$, we can evaluate the exchange contribution to **D**, $\mathbf{D}^{ex}$, by computing the difference $\mathbf{D}^{ex} = \mathbf{D} - \mathbf{D}^d$. According to the two possible choices of sign for **D** we obtain two tensors that, referred to the principal **g** axis system, are

$$\mathbf{D}^{ex}{}_1 = \begin{pmatrix} 0.0124 & -0.0003 & 0.0013 \\ -0.0003 & 0.0039 & 0.0005 \\ 0.0013 & 0.0005 & -0.0164 \end{pmatrix}$$

$$\mathbf{D}^{ex}{}_2 = \begin{pmatrix} 0.0120 & 0.0023 & -0.0128 \\ 0.0023 & -0.0164 & 0.0002 \\ -0.0128 & 0.0002 & 0.0044 \end{pmatrix}$$

Both $\mathbf{D}^{ex}{}_1$ and $\mathbf{D}^{ex}{}_2$ are not diagonal, and it is apparent that the large anisotropy of the observed **D** is due to the off-diagonal elements of $\mathbf{D}^{ex}$.

Third-order perturbation theory allowed Moriya[34] to derive general expressions for $\mathbf{D}^{ex}$, which for two equivalent copper centers become

$$D^{ex}{}_{ij} = \lambda^2 \sum_{e,e'} (\langle g_A|L_i|e_A\rangle \langle e'_A|L_j|g_A\rangle / \Delta_e \Delta_{e'}) J_{e,e',g} \qquad (1)$$

where $|g_A\rangle$ and $|e_A\rangle$ are the ground and excited molecular orbitals localized on copper A and Δ_e is the energy separation between $|e_A\rangle$ and $|g_A\rangle$. $J_{e,e',g} = \langle e_A g_B|H_{ex}|e'_A g_B\rangle = \langle e_B g_A|H_{ex}|e'_B g_A\rangle$ is an exchange integral involving the ground state of one of the ions forming the couple and excited states of the other. In our notation a positive sign for J means antiferromagnetic interaction. Assuming $|g\rangle = |xy\rangle$, which is a good description of the ground state of the present complex, tensor (1) can be written as (2).

$$\begin{pmatrix} (\Delta g_{xx})^2 J_{xz,xz,xy}/8 & (\Delta g_{xx})(\Delta g_{yy}) J_{xz,yz,xy}/2 & (\Delta g_{xx})(\Delta g_{zz}) J_{xz,x^2-y^2,xy}/4 \\ (\Delta g_{xx})(\Delta g_{yy}) J_{xz,yz,xy}/2 & (\Delta g_{yy})^2 J_{yz,yz,xy}/8 & -(\Delta g_{yy})(\Delta g_{zz}) J_{yz,x^2-y^2,xy}/4 \\ (\Delta g_{xx})(\Delta g_{zz}) J_{xz,x^2-y^2,xy}/4 & -(\Delta g_{yy})(\Delta g_{zz}) J_{yz,x^2-y^2,xy}/4 & (\Delta g_{zz})^2 J_{x^2-y^2,x^2-y^2,xy}/32 \end{pmatrix} \qquad (2)$$

Using in (2) the experimental Δg's, we can estimate the $J_{e,e',g}$ integrals from the D^{ex}_{ij} ($i \neq j$) elements. This procedure gives

$$J_{xz,yz,xy} = -0.2\ (1.3) \qquad J_{xz,x^2-y^2,xy} = 0.3\ (-3)$$
$$J_{yz,x^2-y^2,xy} = -0.1\ (-0.4) \tag{3}$$

expressed in cm^{-1}. The values in parentheses in (3) refer to $\mathbf{D}^{ex}_2$. Extracting the $J_{e,e',g}$ integrals from the diagonal elements of $\mathbf{D}^{ex}$ is complicated by the fact that the experimental **D** tensor is traceless and the three principal values are not linearly independent. Assuming an overall C_{2h} symmetry for the dinuclear complex, the four HOMO's of the oxalato molecule[35] span the $A_u + A_g + B_u + B_g$ irreducible representations of the C_{2h} point group (Figure 5). The $|xy\rangle$ and $|yz\rangle$ orbitals on copper span $a_u + b_g$, and $|x^2 - y^2\rangle$ and $|xz\rangle$ span $a_g + b_u$. $J_{yz,yz,xy}$ is expected to be antiferromagnetic (positive sign) due to antiferromagnetic exchange pathways of the type $xy||(A_u + B_g)||yz$, and a ferromagnetic value (negative sign) is anticipated for $J_{xz,xz,xy}$ and $J_{x^2-y^2,x^2-y^2,xy}$ through the exchange pathways $xy||(A_u + B_g) \perp (A_g + B_u)||xz,x^2 - y^2$. This leads in (2) to $D^{ex}_{xx} < 0$, $D^{ex}_{yy} > 0$, and $D^{ex}_{zz} < 0$.

By making (2) traceless, we obtain the diagonal elements of the $\mathbf{D}^e$ tensor to compare with $\mathbf{D}^{ex}_1$ and $\mathbf{D}^{ex}_2$:

$$D^e_{xx} = (2D^{ex}_{xx})/3 - D^{ex}_{yy}/3 - D^{ex}_{zz}/3 \tag{4}$$

$$D^e_{yy} = (2D^{ex}_{yy})/3 - D^{ex}_{xx}/3 - D^{ex}_{zz}/3 \tag{5}$$

$$D^e_{zz} = (2D^{ex}_{zz})/3 - D^{ex}_{xx}/3 - D^{ex}_{yy}/3 \tag{6}$$

Using the signs anticipated for D^{ex}_{ii}, eq 5 requires that $D^e_{yy} > 0$. This condition is matched only by the $\mathbf{D}^{ex}_1$ tensor.

Since (4)–(6) are not linearly independent, it is not possible to uniquely determine D^{ex}_{ii} from the experiment. In series of copper(II) dimers formed by square-planar monomeric units, it was usually found[6,8] that, to a good approximation, $J_{xz,xz,xy} = J_{yz,yz,xy} = 0$ and a ferromagnetic value was measured for $J_{x^2-y^2,x^2-y^2,xy}$. In the present case eq 4 and 5 would require $D^e_{xx} = D^e_{yy} = -D^e_{zz}/3$, which is not observed for either $\mathbf{D}^{ex}_1$ or $\mathbf{D}^{ex}_2$, and we must expect $J_{xz,xz,xy} \neq J_{yz,yz,xy} \neq 0$. This is probably due to the deviation of the copper from the coordination plane observed in the present complex, which lowers the symmetry of the copper coordination environment and is expected to increase the overlap density between the $|xy\rangle$, $|xz\rangle$, and $|yz\rangle$ type molecular orbitals since the $|xy\rangle$ molecular orbital is no longer in a nodal plane of the other two orbitals. In order to estimate, however, the order of magnitude of the exchange interaction, we put in (6) $D^{ex}_{xx} = D^{ex}_{yy} = 0$. By equating (6) to $D^{ex}_{1,zz}$, we get $J_{x^2-y^2,x^2-y^2,xy} = -10$ cm^{-1}.

Conclusions

It is definitely clear that anisotropic exchange interactions are operative in determining the zero-field splitting of exchange-coupled copper(II) complexes. These interactions decrease drastically on increasing the complexity of the molecular groups bridging the two metals from values around 200–300 cm^{-1} for monoatomic bridges[6] to 50 cm^{-1} for N_3^- bridges[9] and 10–30 cm^{-1} for triazoles[10] and oxalates, and EPR spectroscopy is a very sensitive and useful tool to investigate these interactions. This behavior can be qualitatively understood on the basis of density overlap considerations, which demand a decrease of the overlap density on passing from monoatomic to extended bridges, while a quantitative model allowing for an accurate description of the interaction is still lacking. The present results show that even with bridges as extended as the oxalato ones exchange contributions to **D** cannot be neglected and, even if they do not cause significant deviations of the absolute value of D from the value arising from the magnetic dipolar interaction, low-symmetry effects can yield largely misaligned **g** and **D** tensors.

Acknowledgment. Thanks are expressed to Prof. Dante Gatteschi, University of Florence, for helpful discussions. We thank the Centro di Calcolo Elettonico of Modena University for computing facilities and the Ministero della Pubblica Istruzione for grants.

Registry No. $[Cu_2(phen)_2(C_2O_4)(NO_3)_2]$, 106762-40-7.

Supplementary Material Available: Tables of thermal parameters (Table SI) and positional parameters of the hydrogen atoms (Table SII) (2 pages); a table of observed and calculated structure factors (Table SIII) (13 pages). Ordering information is given on any current masthead page.

(34) Moriya, T. *Phys. Rev.* **1960**, *120*, 91.
(35) Verdaguer, M.; Kahn, O.; Julve, M.; Gleizes, A. *Nouv. J. Chim.* **1985**, *9*, 325.

Notes

Contribution from the Institut für Anorganische Chemie and Laboratorium für Kristallographie, Universität Bern, CH-3009 Bern, Switzerland

Synthesis and Crystal Structure of $[Re(bpy)_3](ReO_4)_2$ (bpy = 2,2'-Bipyridine)

Martin Stebler,[1a,b] Alberto Gutiérrez,[1b] Andreas Ludi,[1a] and Hans-Beat Bürgi*[1b]

Received December 10, 1986

The complexes $Ru(bpy)_3^{2+}$ and $Re(bpy)(CO)_3Cl$ and related compounds are widely used as photosensitizers and/or catalysts for the conversion of light into chemical energy.[2] This and the scarcity of structurally characterized mononuclear octahedral Re(II) complexes[3] prompted us to report the synthesis, crystal structure, and some physical properties of air-stable $[Re(bpy)_3](ReO_4)_2$ (**1**), which may serve as a starting material for $Re(bpy)_3^+$, an isoelectronic analogue of $Ru(bpy)_3^{2+}$.

Synthesis

1 was synthesized under a nitrogen atmosphere; 378 mg (1.0 mmol) of K_2ReF_6 was added to a hot solution (85 °C) of 487 mg (3.0 mmol) of 2,2'-bypyridine in 50 mL of H_2O. The resulting clear pink solution was kept at 85 °C for 48 h. During this time the color slowly changed to dark purple. The reaction mixture was then cooled to room temperature, and placed in a refrigerator. Air-stable blue-black, hexagonal prismatic crystals formed, which were collected by filtration, washed with ice-cold water and cold ethanol, and finally dried with ether (yield 30%).

(1) (a) Institut für Anorganische Chemie. (b) Laboratorium für Kristallographie.
(2) See: Balzani, V.; Bolletta, F. *Comments Inorg. Chem.* **1983**, *2*, 211. Seddon, E. A.; Seddon, K. R. *The Chemistry of Ruthenium*; Elsevier: Amsterdam, 1984. Hawecker, J.; Lehn, J. M.; Ziessel, R. *J. Chem. Soc., Chemm. Commun.* **1983**, 536.
(3) A search through the Cambridge Crystallographic Data File revealed the structure of four mononuclear octahedral Re(II) compounds.[16-18]

0020-1669/87/1326-1449$01.50/0